Available online at www.sciencedirect.com
ScienceDirect
Journal of Power Sources 173 (2007) 648–656
JOURNAL OF POWER SOURCES
www.elsevier.com/locate/jpowsour

Interpenetrating ionomer–polymer networks obtained by the *in situ* polymerization in pores of PVdF sponges as potential membranes in PEMFC applications

P. Moszczyński [a], M. Kalita [a,*], P. Parzuchowski [b], M. Siekierski [a], W. Wieczorek [a]

[a] *Polymer Ionics Research Group, Chemical Faculty, Warsaw University of Technology, Noakowskiego 3, PL-00664 Warsaw, Poland*
[b] *Department of Polymer Chemistry and Technology, Chemical Faculty, Warsaw University of Technology, Noakowskiego 3, PL-00664 Warsaw, Poland*

Available online 21 May 2007

Abstract

This article presents studies on novel composite electrolytes having the structure of semi-interpenetrating polymer networks for possible application as an electrolyte in fuel cells. The electrolytes were synthesized by soaking the macroporous Kynar-Flex® (copolymer of vinylidene fluoride and hexafluoropropylene) sponge with water solution of the ionomer followed by the *in situ* free-radical polymerization of the later. Two ionomers having different acidity-methacrylic acid and *p*-styrenesulfonic acid were tested. The ionic conductivity of proposed membranes measured for several systems was high enough for applications in fuel cell in the 20–90 °C temperature range. For higher temperatures, the conductivity decreased because of the membrane drying. The fraction of water in the electrolytes was determined using weight loss analysis. The influence of inorganic filler addition and cross-linking ratio on physicochemical and electrochemical properties of the membranes were also tested.

Keywords: Polymer exchange membrane fuel cell; Semi-interpenetrating polymer networks; Hydrogels; Polymer blends

1. Introduction

It is commonly known that polymer electrolyte fuel cells (PEMFC) are devices which, due to their potential high efficiency, low operating temperature and usage safety [1], can play an important role in energy conversion technology. However, state-of-the-art of the fuel cells technology shows that several problems must have been overcome. When taking into consideration the electrolyte, the main goals are good stability in the potential regime characteristic for the electrodes (or in other words, stability counter oxidation and reduction), proper water management (i.e. membrane humidification being stable and independent of the cell temperature and current load), high and stable ionic conductivity, the simple synthesis and, thus, low production cost as well as low or even non-fuel permeability (in the case of the liquid fuels) [2–4]. The last factor is critical for the application in direct methanol fuel cell (DMFC) for the majority of electrolytes previously used successfully in the hydrogen fuel cells.

A typical example to confirm this observation is Nafion®, which is nowadays used in majority of well-developed or even commercially available hydrogen PEMFC systems. Nafion® is not a barrier material for methanol and, thus, its application in DMFC results in low energetic efficiency due to the so-called methanol cross-over. This phenomenon (leading to the cell voltage decrease) is related to the fact that the methanol is transported through the membrane and oxidized also in the cathode area [5–9]. Both the above mentioned disadvantage and the high production cost of Nafion® encourages the efforts focused on the synthesis of the new materials characterized with both better properties and lower price.

The common synthesis strategy of the materials which can substitute Nafion is based on the sulfonation of previously obtained non-ionomeric polymer [10–13]. Membranes produced on the basis of this approach are commercially available (e.g. sulfonated copolymer of α,α,β-trifluorostyrenes (BAM) [14,15] and sulfonated terpolymer of butylene, ethylene and styrene (SEBS) [16–18]). Sulfonation compounds which are in typical use comprise of sulfur trioxide SO_3, chlorosulfonic acid $ClSO_3H$, sulfuryl chloride SO_2Cl_2 and, for some compounds, sulfuric acid. This route leads to the introduction of the additional step in the synthesis process. Due to the degra-

* Corresponding author. Tel.: +48 22 6605739; fax: +48 22 6282741.
E-mail address: michalka@soliton.ch.pw.edu.pl (M. Kalita).

0378-7753/$ – see front matter © 2007 Elsevier B.V. All rights reserved.
doi:10.1016/j.jpowsour.2007.05.064

dation process, a decrease of the molecular weight of polymer is observed during the sulfonation and the material obtained is usually not homogenous in terms of the sulfonic group density. The additional disadvantage of the compounds used is related to their high chemical aggresivity and, thus, their application to the synthesis of PEMFC membranes should be limited. Moreover, the non-sulfonated polymer precursors are often expensive and obtained materials exhibit poor processability.

Typical micromorphology of the polymer electrolyte applied in fuel cells consists of areas of both hydrophobic (which are responsible for the mechanical of the material) and hydrophilic (which are responsible for charge carriers transport) character. A number of different composite architectures leading to the results in the terms of the microstructure of membrane such as polymer blends [19–21], block copolymers [22,23] as well as organic–inorganic systems [24–26] were tested. A new approach to the synthesis of a low-cost proton-exchange composite membrane (C-PEM) based on PVdF and silica with surface-anchored sulfonic acid (SASA) groups, is presented by Peled and co-workers [27]. The room-temperature conductivity of SASA-based C-PEMs, is in the range of 2.0–50 mS cm^{-1}. The membrane is thermally stable up to 250 °C. Direct methanol fuel cells (DMFCs) have been assembled with some of the membranes. Preliminary tests show that the cell resistance with a non-optimized membrane is in the range of 3 Ω cm^{-2}, therefore the maximum cell power density achieved so far does not exceed 32 mW cm^{-2} at 70 °C. Also a class of systems containing unbound inorganic acid, ceramic filler and polymers [28] or polymer blends as a hydrophobic matrix in their structure was also examined exhibiting high initial ionic conductivity, however, rinsing of the acid from polymer pores is observed during the cell work, leading finally to the unacceptable performance losses [29]. The usage of nanoporous proton-conducting membrane (NP-PCM) based in similar approach but using PTFE [30,31] bring some interesting improvements.

To avoid this problem, we have concentrated on semi-interpenetrating polymer networks (semi-IPN) obtained by free-radical *in situ* polymerization of vinyl monomers containing acid groups in their structure in the pores of the hydrophobic polymeric sponges. While PEMFC electrolytes obtained by grafting of acidic groups or polymers containing acidic groups on hydrophobic polymeric matrices (leading to linear or comb-like structures) were widely studied [32–36], the conception of semi-IPN architecture is quite novel. Using this approach, the rinsing of the acidic groups is inhibited. Moreover, the polymeric structure of the hydrophilic areas should result in better mechanical properties of the membrane in comparison with the systems containing inorganic acid addition. Studies based on a similar approach were conducted by Prakash et al. [37]. Obtained membranes had much lower methanol cross-over rates in comparison with Nafion 117. Due to this, PVdF–PSSA systems gave higher cell voltages and higher power densities then Nafion 117 ones. The main disadvantage of the proposed synthetic path was the usage of $ClSO_3H$ in the additional step of styrene sulfonation after obtaining polystyrene-poly(vinylidene fluoride) semi-IPN. Thus, we tried to synthesize similar systems using water as a solvent and omiting the polymer sulfonation by the use of monomers having acidic groups in their molecular structure.

2. Experimental

2.1. The synthesis of PVdF–HFP copolymer sponges

The PVdF–HFP copolymer (Kynar-Flex®, Arkema) was dissolved in the mixture of 6.5 ml of acetone (pure, POCH) and 1.12 ml of 1-butanol (pure, POCH). After 15 min of intensive stirring the solution was cast on the glass plate and 20 ml of distilled water were added. This resulted in obtaining of a self-standing sponge of good flexibility. The obtained membrane was dried under vacuum to remove residual water, acetone and 1-butanol.

2.2. The synthesis of the electrolyte

The sponges were soaked using the excess of the water solutions containing the monomer, a thermal free-radical initiator (sodium persulfate, $Na_2S_2O_8$, pure p.a., POCH) and (when used) a cross-linking agent (bisacrylamide, BAA, purum, ≥98.0%, Fluka). Four monomers: sodium *p*-styrenesulfonate (SSNa hydrate, Aldrich), sodium *p*-vinylsulfonate (VSNa, 25 wt.% in H_2O, technical grade, Aldrich), methacrylic acid (MAA, purum, Fluka) and acrylic acid (AA, purum, anhydrous, ≥99.0%, Fluka), were used. The reaction conditions and respective compositions of the soaking solutions (as mass ratios) are gathered in Table 1. The fumed silica (powder, 0.007 μm, Sigma) concentration was described as its mass ratio to the monomer while the fraction of the cross-linking agent was calculated as its molar ratio to the monomer.

2.3. Conductivity measurements

An Atlas 98HI Frequency Response Analyzer was used in 1 Hz–100 kHz frequency range. The cell was immersed in a MLW thermostat model U10 to control the measurement temperature in 293–373 K range. Bernard Boukamp EQ software [38] was used for analysis of the obtained impedance data.

To study the stability of the ionic conductivity over-time, the conductivity measurements were performed just after synthesis, and after 1, 2, 4, 8, 16 and 32 days annealing in water. All these measurements were performed at room-temperature (25 °C). For each experiment, a new fragment of the synthesized membrane was used. Simultaneously, with each conductivity measurement,

Table 1
Mass proportions of reagents and reaction conditions

Monomer	Reaction temperature (°C)	Reaction time (h)	Monomer:water (w/w)	Initiator:water (w/w)
SSNa	90	24	1:3	1:100
VSNa	80	24	1:7	1:700
AA	55	2	1:9	1:450
MAA	80	2	1:9	1:450

the water in which the membrane was stored, was exchanged to a fresh portion of water.

2.4. Weight loss measurements

Weight loss (WL) curves registration was performed using Q-1500 D Derivatograph (MOM Budapest) with heating rate of 10 °C min^{-1}. The WL for the membranes was measured twice: just after the synthesis and after 32 days of the storage in the water. In the later case, the water exchange was realized analogically with the conductivity measurements.

2.5. SEM

SEM images was performed using FEI Quanta 200 microscope. The low vacuum mode was used for image gathering. The membranes were dried at 60 °C for at least 6 h under vacuum before the measurement.

3. Results

The goal of the presented work is to synthesize a composite membrane by the *in situ* polymerization of the acidic monomer in the pores of the hydrophobic sponge. In the first stage, the process was optimized to obtain the best hydrophobic construction material for further in situ polymerization. The tests showed that the systems containing vinylidene fluoride (VdF)-hexafluoropropylene (HFP) copolymer (Kynar, Kynar-Flex®) exhibited the best properties. Commercially available PTFE membranes, as Gore-Tex®, are hydrophobic and have too small pores (Fig. 1) to introduce water or even dioxane solution of the ionomer precursors. Contrary to this, Kynar based sponges can be easily soaked with them. Additionally, Kynar exhibits better processibility in comparison with HDPE or PTFE, i.e. solubility in several solvents and good mechanical properties such as flexibility (in comparison to VdF homopolymer). Moreover, by the modification of the process parameters it is possible to obtain Kynar sponges with controlled and well-defined pores size. In the second step the polymerization process was realized in the free-radical regime. Preliminary studies showed that membranes obtained by polymerization of MAA and SSNa are significantly more stable than those of AA and VSNa, respectively, in terms of humidity, ageing and heating. Moreover, the conductivity of MAA- and SSNa- containing systems were not lower than in respective AA- and VSNa- containing ones. Thus, we concentrated on MAA- and SSNa- containing systems.

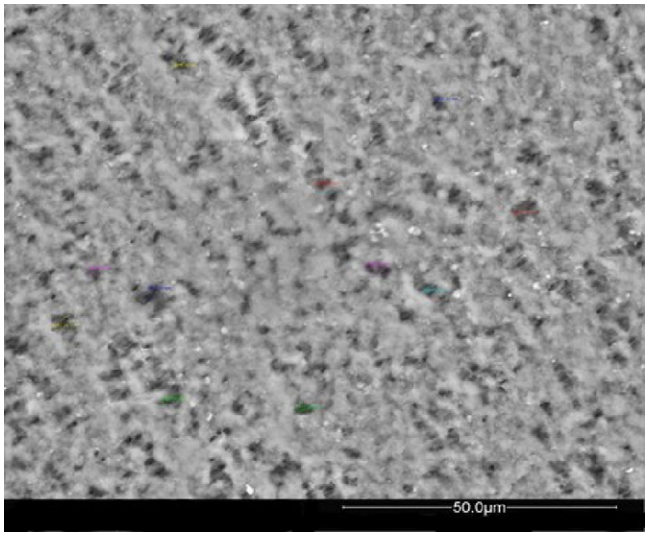

Fig. 1. An SEM image of the Gore-Tex® (Al Gore) membrane.

3.1. MAA–Kynar-based systems

3.1.1. Conductivity measurements

Thermal dependencies of conductivity for membranes characterized with different cross-linking ratios are depicted in Fig. 2. As one can easily see, the highest conductivities are observed for the not cross-linked membranes. Between ambient temperature and 60 °C the conductivity of the membranes increases. Above this temperature, a decrease of the conductivity value is observed which can be attributed to the membrane drying at elevated temperatures. Upon cross-linking a significant deterioration of the membrane resistivity to the drying process is observed. Non-cross-linked materials and these with very small cross-linking ratio behave similarly (still with the favor for the pristine material), while for the strongly cross-linked membranes a conductivity loss threshold is located about 20 ° lower.

To study the stability of the obtained materials against conductivity loss in the water, we conducted the studies in which conductivity changes in time (Fig. 3) were evaluated. The average decrease of the conductivity observed in 32 days period is lower than one order of magnitude. We suggest that this phenomenon can be mainly the result of the additional membrane humidification (membranes swell in water), leading to the decrease of the effective concentration of the acidic group. The additional mechanism giving the same effect can be related to the partial recrystallization of the ionomeric chains which can reduce the mobility of the protons. This observation is valid especially for the poly(methacrylic acid) containing composites in which carboxylic groups can strongly interact with themselves by the formation of the hydrogen bonds.

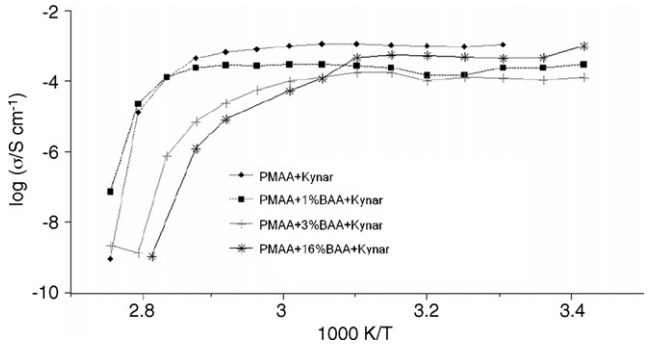

Fig. 2. Thermal dependency of conductivity in PMAA–BAA–Kynar systems.

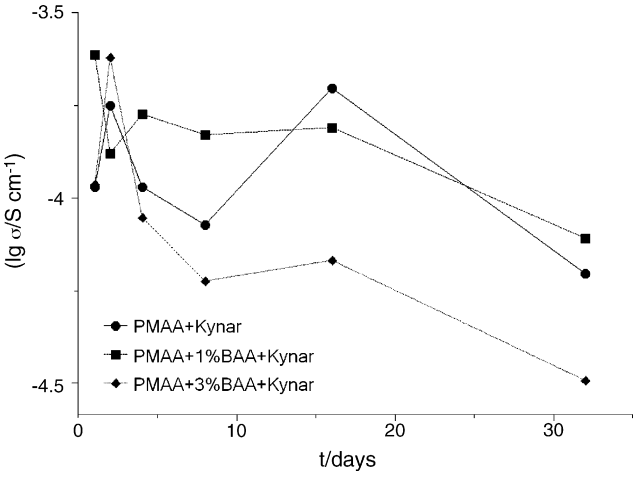

Fig. 3. Conductivity changes as a function of time in PMAA–BAA–Kynar systems.

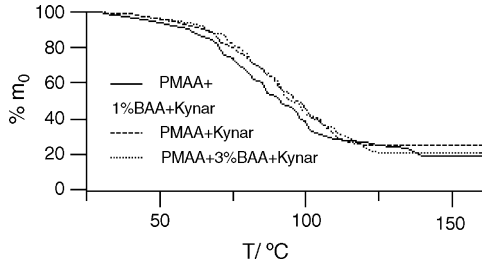

Fig. 4. WL curves—PMAA–BAA–Kynar systems.

3.1.2. WL measurements

The WL curves registered for membranes just after the polymerization reaction characterized with different cross-linking ratios are depicted in Fig. 4. In all cases, the weight loss begins at 60 °C. This observation is in good agreement with the thermal dependency of conductivity. Additionally, at temperatures higher than 120 °C the mass loss curves flatten at the level of about 25% of initial mass. It is because polymer is completely dried. For the cross-linked membrane the weight loss is even higher and the residual weight is equal to only 20% of the initial one.

Experiments conducted 32 days after synthesis (Fig. 5) revealed that the mass loss has a similar character as in the case of the freshly synthesized composite. The only significant difference we observe is that completely dried membranes have a

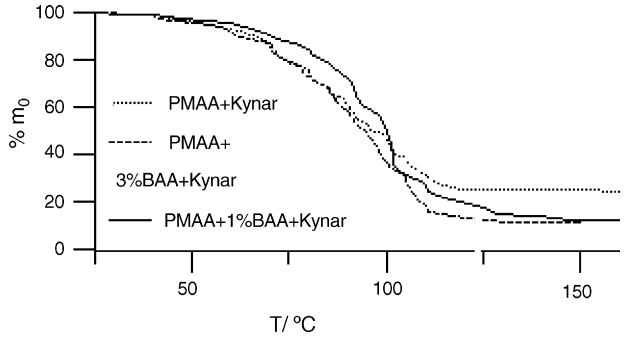

Fig. 5. WL curves—PMAA–BAA–Kynar systems after 32 days of ageing.

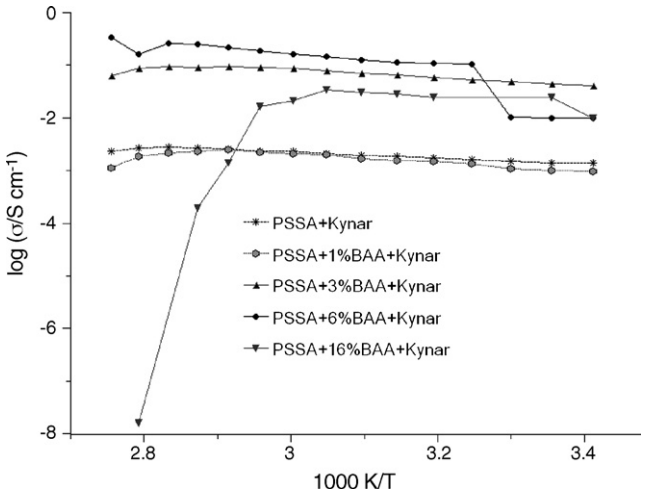

Fig. 6. Thermal dependency of conductivity for PSSA–BAA–Kynar systems.

much lower mass. Better membrane humidification after storage in water leads to increase water content up to 85%.

3.2. PSSA–Kynar-based systems

3.2.1. Conductivity measurements

Thermal dependencies of conductivity of poly(*p*-styrenesulfonic acid)-bisacrylamide systems with various cross-linking ratio are depicted in Fig. 6. For nearly all samples the dependence can be divided into two areas differing with the conductivity change direction. At lower temperatures the conductivity value increases according to the Arrhenius type of dependency with the activation energy similar to the one characteristic for water solution of strong acids ($E_a \cong 10\,\text{kJ mol}^{-1}$). For samples with relatively high cross-linking ratio, the activation energy is significantly higher (see Table 2). Contrary to this, for all samples, in temperature range above 90 °C, conductivity decreases due to the membrane drying.

The studies of conductivity change in time (Fig. 7) showed that conductivity decreases from 10^{-1} to $10^{-2}\,\text{S cm}^{-1}$ to about 10^{-3} to $10^{-4}\,\text{S cm}^{-1}$. Such a strong change cannot be attributed to the water intake by the membrane but is rather related to the rinsing of the low molecular weight SSA olygomers.

3.2.2. WL measurements

The WL curves registered for membranes just after their synthesis (Fig. 8) shows that water loss in the membrane is much slower then in the case of the PMAA-based ones. The mass loss begins in 80 °C and the curve does not flatten up to 160 °C. At

Table 2
Activation energies of conductivity for PSSA–BAA–Kynar systems

System	E_a (kJ mol^{-1})
PSSA	11
PSSA + 1% BAA	16
PSSA + 3% BAA	15
PSSA + 6% BAA	21
PSSA + 16% BAA	22

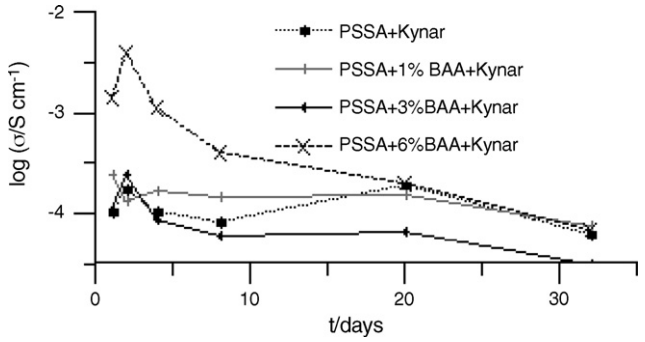

Fig. 7. Conductivity changes as a function of time in PSSA–BAA–Kynar systems.

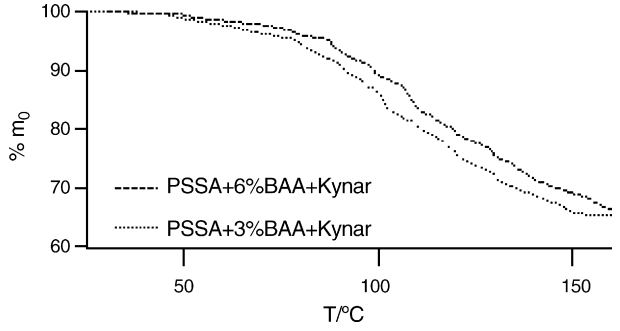

Fig. 8. WL curves—PSSA–BAA–Kynar systems.

this temperature the experiments were finished due to possible PSSA decomposition. The average membrane mass at this temperature is above 60% of initial one, and is much higher than in the case of PMAA-based membranes.

The results of the WL measurements conducted 32 days after the composite synthesis (Fig. 9) differs from those conducted just after it. It can be observed that humidification of the membrane after storage in water is about four times higher (dry membrane to initial mass ratio is equal to 65:100 for the material just after synthesis and to 15:100 after 32 days of storage).

3.3. PMAA–SiO_2–Kynar-based systems

3.3.1. Conductivity measurements

Thermal dependencies of conductivity for these systems and the conductivity change in time are depicted in Figs. 10 and 11, respectively. The conductivity values of these systems at temperatures up to 60 °C are similar or slightly lower in comparison with these not containing ceramic filler. A significant change can be observed at elevated temperatures where the conductivity decrease is smaller than in filler-free ones. Despite the fact that the SiO_2 addition (40%) leads to much better thermal stability of conductivity a time dependent decrease is also diminished and the conductivity does not change with the time of the membrane storage in water.

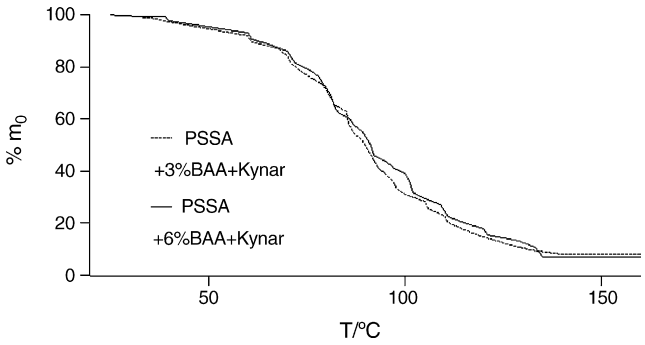

Fig. 9. WL curves—PSSA–BAA–Kynar systems after 32 days of ageing.

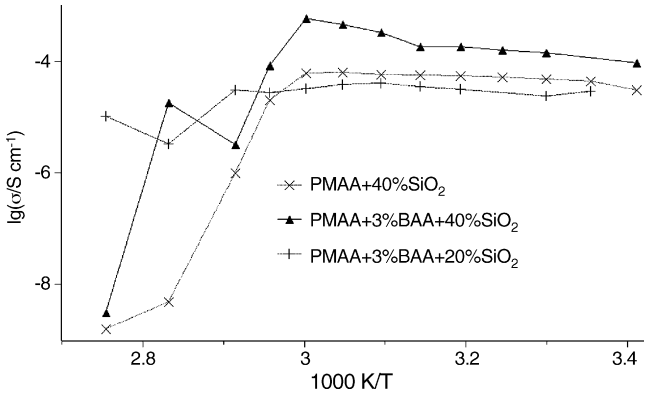

Fig. 10. Thermal dependency of conductivity for PMAA–BAA–SiO_2–Kynar systems.

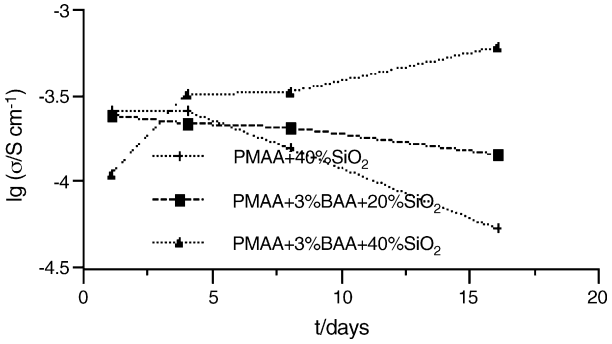

Fig. 11. Conductivity changes as a function of time in PMAA–BAA–SiO_2–Kynar systems.

3.3.2. WL measurements

The WL curves for these systems (Fig. 12) reveal that the membrane humidification for cross-linked membranes is much higher than in the membranes with no ceramic filler addition and

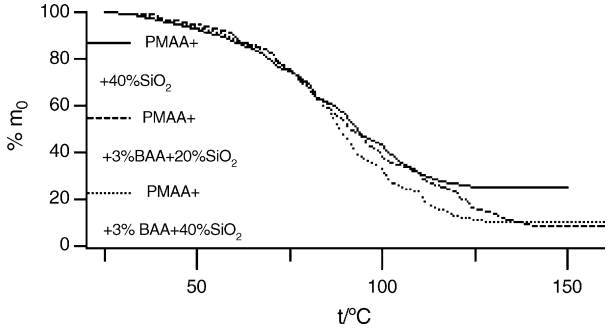

Fig. 12. WL curves—PMAA–BAA–SiO_2–Kynar systems.

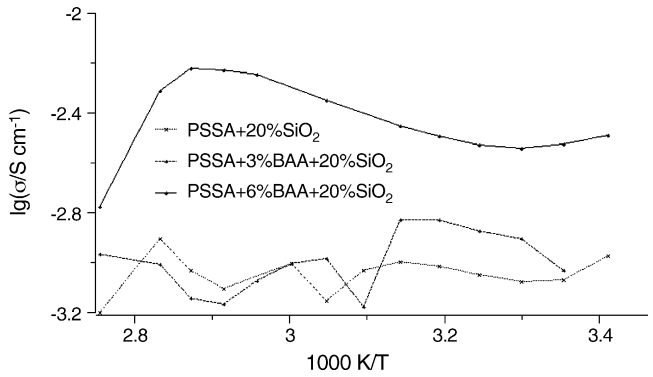

Fig. 13. Thermal dependency of conductivity for PSSA–BAA–SiO_2–Kynar systems.

the same cross-linking ratio (water:dry membrane mass ratio is about 92:8 for membranes with ceramic filler addition, for filler-free it is about 65:35). Contrary to this, the composite containing not cross-linked PMAA behaves differently. In this case, the residual mass is equal to 25% of the initial one, so to the value typical to the systems not containing ceramic filler.

3.4. PSSA–SiO_2–Kynar-based systems

3.4.1. Conductivity measurements

Thermal dependencies of conductivity for these systems are presented in Fig. 13. One can observe that the ceramic filler addition in the case of membrane containing not cross-linked PSSA, opposite to PMAA–SiO_2-based one, results in the decrease of the threshold temperature for the conductivity depletion. This phenomenon should be related to easier membrane drying. The conductivity lowering was observed in 70 °C whereas in filler-free membrane the conductivity was stable up to 90 °C. Additionally, the addition of the ceramic filler to the membrane with the ionomeric part consisting of the cross-linked PSSA results in the lowering of conductivity by about two orders of magnitude. The studies of conductivity change in time (Fig. 14) reveal that the ceramic filler addition does not prevent PSSA from being rinsed from the pores of the Kynar® matrix. This observation is also contrary to the stabilization phenomenon which was observed for the PMAA–SiO_2-based composites.

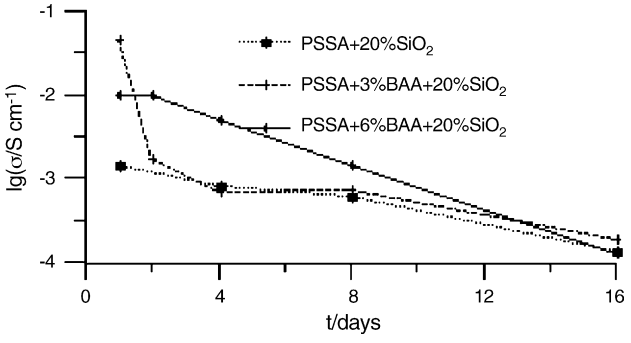

Fig. 14. Conductivity changes as a function of time in PSSA–BAA–SiO_2–Kynar systems.

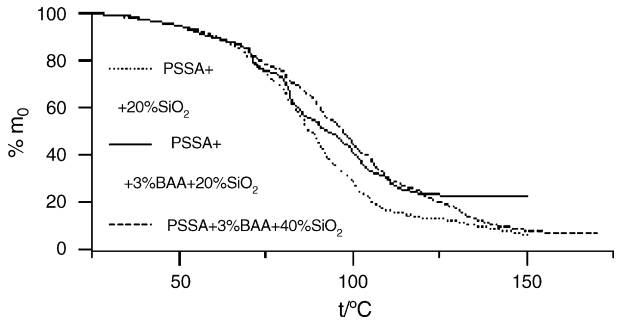

Fig. 15. WL curves—PSSA–BAA–SiO_2–Kynar systems.

3.4.2. WL measurements

The WL curves are presented in Fig. 15. As one can easily observe, the mass loss in these systems begins in temperatures lower than 50 °C. These results show the thermal stability loss in comparison with the ceramic filler-free systems in which the significant mass loss begins above 100 °C. On the other hand, both the non-cross-linked material with 20% of SiO_2 and the cross-linked composite with higher (40%) ceramic filler addition revealed a very high water content (dry membrane to initial mass ratio is only 8:100) while for the one with the lower grain content (20%) and the cross-linked ionomeric part water content is significantly lower (about 80%).

3.5. SEM images

The SEM images of the PMAA-containing systems are depicted in Figs. 16 and 17 (without and with ceramic filler addition, respectively). In the case of filler-free membrane, one can observe a laminar smooth structure copying the surface of the Teflon substrate on which the membrane synthesis was held. Contrastively the image of filler containing membrane shows that a core–shell-like structures are formed with the added grains being the agglomeration centers.

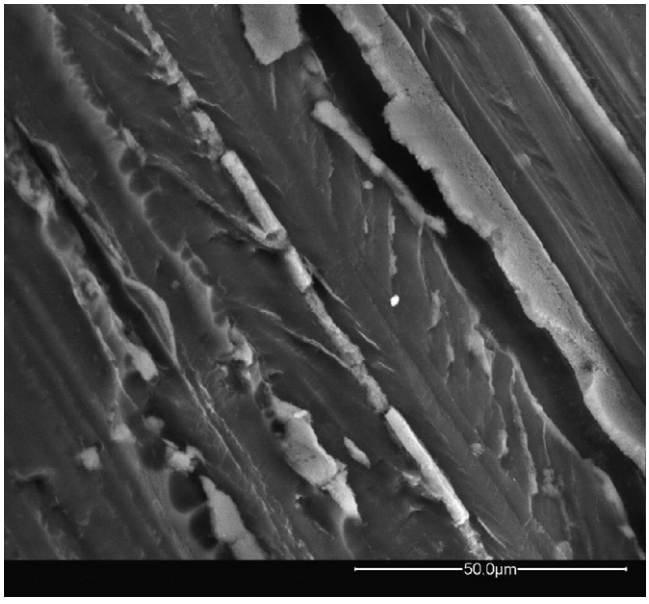

Fig. 16. SEM image of the PMAA + 1% BAA system (magnitude 1300×).

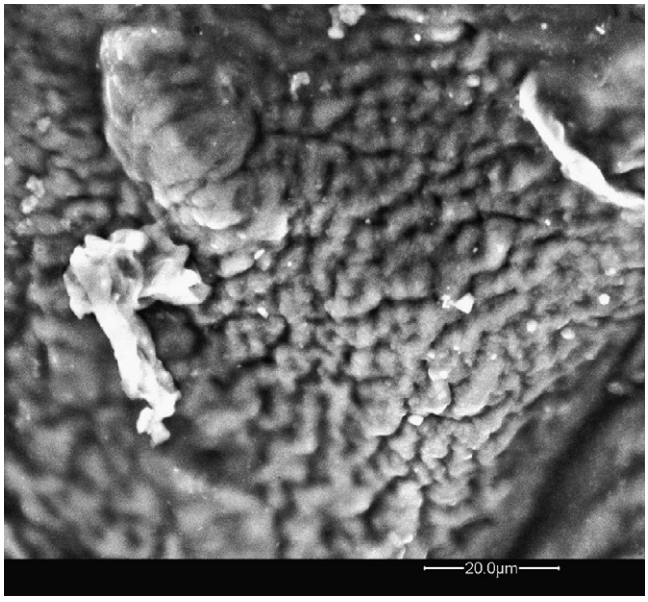

Fig. 17. SEM image of the PMAA + 3% BAA + 20% SiO_2 system (magnitude 1600×).

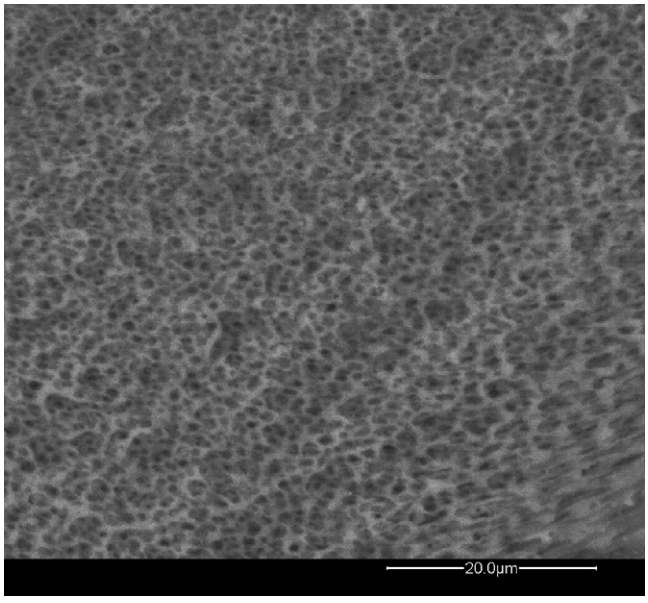

Fig. 18. SEM image of the PSSA system (magnitude 2500×).

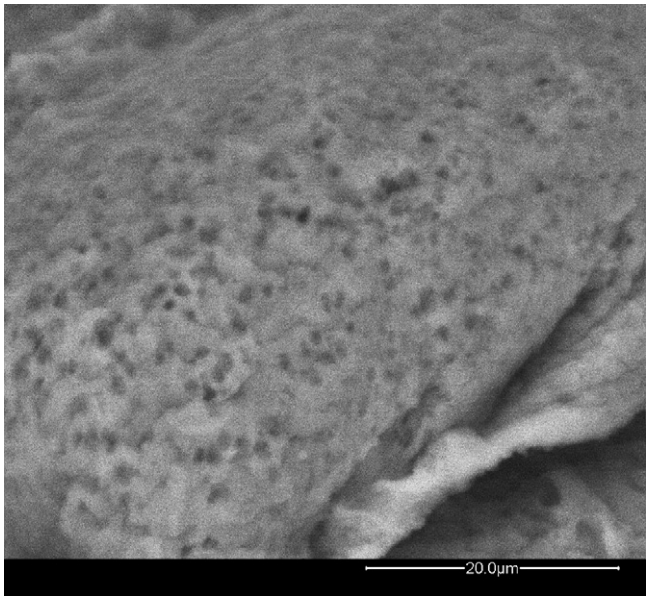

Fig. 19. SEM image of the PSSA + 6% BAA system (magnitude 3000×).

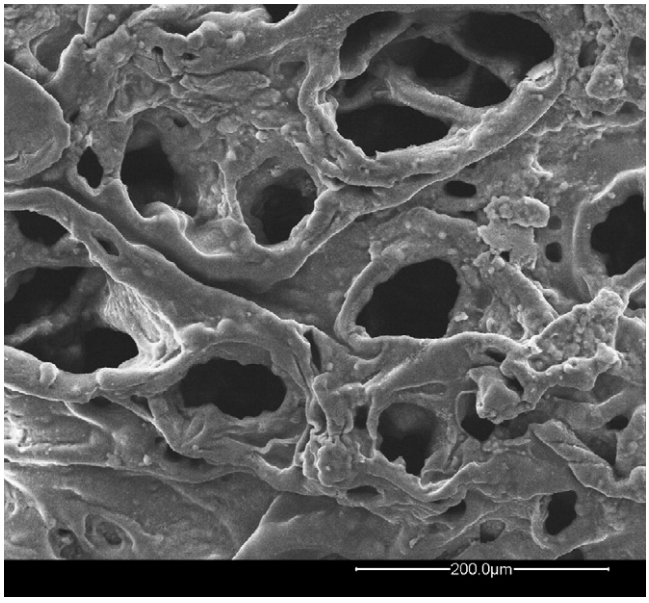

Fig. 20. SEM image of the PMAA + 6% BAA + 20% SiO_2 system (magnitude 300×).

The images of the PSSA-containing systems are presented in Figs. 18 and 19. In these systems one can observe a microporous structure. The addition of the cross-linking agent does not change the membrane morphology significantly. In this case the ceramic filler addition (SEM image presented in Fig. 20) leads to obtaining the membrane in which the macroporous structure of the PVdF sponges is obtained.

.

4. Discussion

The ceramic filler addition improves the properties of PMAA-based composites, whereas a similar effect in not observed in PSSA. We suggest that it is due to the stronger interactions between acidic groups in MAA-containing composites in comparison to the ones observed for sulfonic groups in the SSA-containing composites. This phenomenon can be attributed to the fact that two carboxyl groups–COOH in PMAA can form a much stronger double hydrogen bond (see Fig. 21). The sulfonic group hydrogens are much more acidic in comparison with the

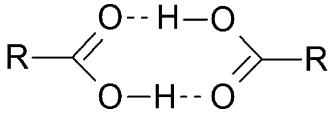

Fig. 21. Double hydrogen bond formed by two carboxyl groups.

ones belonging to the carboxyl groups and, thus, they are dissociated to a larger ratio. Therefore, the ceramic filler is not able to further improve the ionic equilibrium in SSA-containing composites whereas for the MAA-containing ones an improvement of dissociation can be observed leading to the conductivity increase.

Another reason of these changes is changes in the membrane morphology. In the PMAA-containing systems we observe formation of the core–shell-like structures. This organization of the molecules can thus lead to the formation of the fast conducting paths. In the case of the PSSA-containing membranes the ceramic filler addition results in the material microstructure degradation leading to the worse polymer matrix-hydrogel compatibility. In consequence make the obtained ionomer can be easily washed out what leads to the faster conductivity deterioration during seasoning in water.

In PMAA-based composites the maximum of the conductivity is observed for membrane containing not cross-linked PMAA. For this system, a strong physical cross-linking is observed between the polymeric chains of the homopolymer and even the non-cross-linked system behaves as a gel. Therefore, the additional covalent cross-linking is unnecessary and leads to a conductivity decrease due to the additional chain mobility depletion. Contrary to this, in PSSA-based systems maximum conductivity was observed for membranes in which cross-linking agent: monomer ratio was equal to 3:100 and 6:100. This last result is in good agreement with work of Prakash et al. [37]: in system he studied this maximum was observed for membranes having divinylbenzene: styrene ratio between 4:100 and 10:100.

5. Conclusions

The properties of strongly humidified composite electrolytes based on polymeric blends were tested. It was proved that it is possible to synthesize materials which have high ionic conductivity by the *in situ* polymerization of the ionomer precursor. In comparison to the majority of systems known from literature, this synthetic path was much easier to conduct and the reagents used were commercially available and relatively cheap. Contrary to the non-blended hydrogels, the obtained membranes are characterized with good mechanical stability.

We also prove that the properties of the studied systems can be modified by the addition of the ceramic filler and/or cross-linking compound. We suggest that similar systems can be also modified by the addition of the comonomer to the ionomer solution. Moreover, for the construction polymer in the form of the macroporous sponge, no problems related to the introduction of the nanosized ceramic filler can be observed due to the fact that the filler suspension in water easily penetrates the pores.

Thermal dependencies on conductivity suggest that mechanism of the conductivity of the studied systems is similar to that observed in water solutions of mineral acids. It is in good agreement with the WL studies which revealed that in majority of systems studied the water content is higher than 80% (or even 90%) of the overall mass of the composite.

Finally, we suggest that from the tested systems the PMAA–SiO_2–PVdF one upon the obtained data exhibits long enough conductivity stability and small enough water loss in elevated temperatures to be qualified for preliminary tests in PEMFC. Contrary, the PSSA-based systems do not show good enough properties for the practical applications even exhibiting higher initial room-temperature conductivity value.

Acknowledgements

The presented research was financially supported by Warsaw University of Technology. Mr. Andrzej Łukaszewicz is kindly acknowledged for the proofreading of the manuscript. PM thank Prof. Gabriel Rokicki for allowing to work in his team laboratory and Ing. Roland Witak for WL curves registration. MK acknowledges Ph.D. Leszek Łukasik for helpful comments and fruitful discussions.

References

[1] M.A. Hickner, H. Ghassemi, Y.S. Kim, B.R. Einsla, J.E. McGrath, Chem. Rev. 104 (2004) 4587.
[2] N.P. Brandon, S. Skinner, B.C.H. Steele, Annu. Rev. Mater. Res. 33 (2003) 183.
[3] M. Rikukawa, K. Sanui, Prog. Polym. Sci. 25 (2000) 1463.
[4] O. Savadogo, J. New Mater. Electrochem. Syst. 1 (1998) 47.
[5] K.M. McGrath, G.K.S. Prakash, G.A. Olah, J. Ind. Eng. Chem. 10 (2004) 1063–1080.
[6] J. Kallo, W. Lehnert, R. von Helmolt, J. Electrochem. Soc. 150 (2003) A765–A769.
[7] J. Ling, O. Savadogo, J. Electrochem. Soc. 151 (2004) A1604–A1610.
[8] V.M. Barragan, C. Ruiz-Bauza, J.P.G. Villaluenga, B. Seoane, J. Power Sources 130 (2004) 22–29.
[9] A. Heinzel, V.M. Barragan, J. Power Sources 84 (1999) 70–74.
[10] H.C. Lee, H.S. Hong, Y.-M. Kim, S.H. Choi, M.Z. Hong, H.S. Lee, K. Kim, Electrochim. Acta 49 (2004) 2315–2323.
[11] J.A. Asensio, S. Borros, P. Gomez-Romero, Electrochim. Acta 49 (2004) 4461–4466.
[12] C. Hasiotis, V. Deimede, C. Kontoyannis, Electrochim. Acta 46 (2001) 2401–2406.
[13] H. Ghassemi, J.E. McGrath, T.A. Zawodzinski Jr., Polymer 47 (2006) 4132–4139.
[14] S.A. Weiner, J. Power Sources 71 (1998) 61–64.
[15] T.R. Ralph, G.A. Hards, J.E. Keating, S.A. Campbell, D.P. Wilkinson, M. Davis, J. StPierre, M.C. Johnson, J. Electrochem. Soc. 144 (1997) 3845–3857.
[16] D.E. Winkler, US Patent 3,577,357 (1971).
[17] B. M. Sheikh-Ali, G. E. Wnek, US Patent 6,110,616 (2000).
[18] C.A. Edmondson, J.J. Fontanella, S.H. Chung, S.G. Greenbaum, G.E. Wnek, Electrochim. Acta 46 (2001) 1623.
[19] H.-Y. Cho, J.-Y. Eom, H.-Y. Jung, N.-S. Choi, Y.-M. Lee, J.-K. Park, J.-H. Choi, K.-W. Park, Y.-E. Sung, Electrochim. Acta 50 (2004) 583.
[20] M.-K. Song, Y.-T. Kim, J.M. Fenton, H.R. Kunz, H.-W. Rhee, J. Power Sources 117 (2003) 14.
[21] J. Lin, J.K. Lee, M. Kellner, R. Wycisk, P.N. Pintauro, J. Electrochem. Soc. 153 (2006) A1325.
[22] Y. Yang, Z. Shi, S. Holdcroft, Macromolecules 104 (2004) 1678.
[23] Z. Shi, S. Holdcroft, Macromolecules 38 (2005) 4193–4201.
[24] S. Panero, P. Fiorenza, M.A. Navarra, J. Romanowska, B. Scrosati, J. Electrochem. Soc. 152 (2005) A2400.
[25] M.A. Navarra, S. Materazzi, S. Panero, B. Scrosati, J. Electrochem. Soc. 150 (2003) A1528.
[26] A. Martinelli, M.A. Navarra, A. Matic, S. Panero, P. Jacobsson, L. Borjesson, B. Scrosati, Electrochim. Acta 50 (2005) 3992–3997.

[27] T. Duvdevani, M. Philosoph, M. Rakhman, D. Golodnitsky, E. Peled, J. Power Sources 161 (2006) 1069.
[28] E. Peled, T. Duvdevani, A. Melman, J. Electrochem. Solid State Lett. 1 (1998) 210.
[29] B. Scrosati, M.A. Navarra, A. Fernicola, S. Panero, ECS Trans. 1 (6) (2005) 169–174.
[30] A. Blum, T. Duvdevani, M. Philosoph, N. Rudoy, E. Peled, J. Power Sources 117 (2003) 22.
[31] E. Peled, V. Livshits, T. Duvdevani, J. Power Sources 106 (2002) 245.
[32] B. Soresi, E. Quartarone, P. Mustarelli, A. Magistris, G. Chiodelli, Solid State Ionics 166 (2004) 383–389.
[33] C. Chuy, V. Basura, E. Simon, S. Holdcroft, J. Horsfall, K. Lovell, J. Electrochem. Soc. 147 (2000) 4453.
[34] S. Flint, R. Slade, Solid State Ionics 97 (1997) 299.
[35] M.M. Nasef, N.A. Zubir, A.F. Ismail, M. Khayet, K.Z.M. Dahlan, H. Saidi, R. Rohani, T.I.S. Ngah, N.A. Sulaiman, J. Membr.Sci. 268 (2006) 96–108.
[36] K.-Y. Cho, H.-Y. Jung, N.-S. Choi, S.-J. Sung, J.-K. Park, J.-H. Choi, Y.-E. Sung, Solid State Ionics 176 (2005) 3027–3030.
[37] G.K.S. Prakash, M.C. Smart, Q.-J. Wang, A. Atti, V. Pleynet, B. Yang, K. McGrath, G.A. Olah, S.R. Narayanan, W. Chun, T. Valdez, S. Surampudi, J. Fluorine Chem. 125 (2004) 1217–1230.
[38] B.A. Boukamp, Solid State Ionics 10 (1986) 31.